Stochastic Optimization for Energy Management in Power Systems with Multiple Microgrids

Shasha Wang, Harsha Gangammanavar, Sandra D. Ekşioğlu, and Scott J. Mason

***Abstract*—This work is motivated by a power system with one main grid (arbiter) and multiple mirogrids (agents). The microgrids (MGs) are equipped to control their local generation and demand in the presence of uncertain renewable generation and various energy management settings. We propose an extension to the two-stage stochastic programming model to capture the interactions between the main grid and MGs. This model includes multiple agents with decisions and stochastic processes in the second-stage. To tackle this problem, we use sequential sampling-based optimization methods that do not require a priori knowledge of probability distribution functions or selection of samples for renewable generation. Therefore our solution approach, which we call the multi-agent stochastic decomposition, can be used in conjunction with simulators and is amenable for distributed computing environments. Our computational experiments conducted on the US western interconnect (WECC-240) data set reveal that the proposed algorithm is scalable and the solutions found are statistically verifiable. Our results also indicate that the proposed energy management system guarantees an efficient utilization of renewable resources.**

I. Introduction

Microgrids have recently emerged as an alternative for reducing greenhouse gas emissions and transmission losses [1], [2]. A microgrid (MG) is a small-scale power grid that is comprised of distributed energy resource systems, storage devices, local demands, and a distribution network [3], [4]. The capacity of such a distributed energy resource system varies from 1500 kW to 1000 MW, which is smaller than a centralized conventional power station [5]. Although gas, diesel, fuel oil, biogas/biodiesel, wind, and solar can all be used as energy resources in an MG [6], MGs offer an ideal setting for distributed generation, which is mostly comprised of renewable energy resources [7]–[11]. For example, the second largest island in the US, Kodiak, Alaska, has an average annual 99.7% renewable energy penetration. However, the inherent stochasticity of renewable resources, such as wind and solar, introduces operational challenges in such MGs.

An attractive feature about MGs is their ability to operate both as part of a larger power grid as well as in an islanded mode. The MGs can transact power with the larger grid when they are connected, thereby acting as a source/sink for deficient/excess power in the system. In times of stress, such as during a storm or service interruption, an MG can break off from the larger grid and operate independently on its own. These capabilities can provide additional reliability options to power system operations. In addition, MGs provide favorable settings to enable flexible energy management solutions.

For these reasons, there has been a growing number of publications that focus on the operations of MGs. Su *et al.* [12] analyze a two-stage stochastic programming problem of energy management in a single MG with renewable resources. Nguyen and Le [4] present a scenario-based two-stage stochastic optimization framework for energy management in a cooperative network of MGs. The problem is formulated as a large-scale, mixed-integer linear program, which is solved by CPLEX. Wang *et al.* [13] study a stochastic, bi-level optimization problem that considers coordinated control of networked MGs in the presence of renewable resources. A mathematical program with complementarity constraints and a scenario reduction method are applied to analyze the proposed problem. In both these studies, the authors attempt to optimize all MGs simultaneously, which can result in a large-scale optimization problem. In order to achieve computational viability, they consider only a small number of MGs in the system and resort to a limited sample representation of uncertainty. However, it is expected that in the future, the main grid will interact with a large number of MGs. Further, a limited sample representation of uncertainty in power systems often results in suboptimal solutions and unreliable cost estimates as demonstrated in [14] in the context of economic dispatch. In this regard, a computational optimization framework that addresses the need for scalability and accurate representation of uncertainty is required.

MGs allow combining smart grid control systems and innovative energy management technologies with traditional operations. In a smart grid, customers are allowed to adjust their energy consumption according to real-time electricity prices. The adjustable appliances either have flexible ranges of power demand or can shift their demand between periods. This behavior, which is called demand response, brings operational flexibility while imposing newer challenges on energy management systems. Ding *et al.* [15] propose a scheme to divide processing tasks in industrial facilities into nonschedulable and schedulable tasks. Goddard *et al.* [16] study heating, ventilation, and air conditioning demand response control in commercial buildings. Li *et al.* [17] present detailed models of appliances commonly used in households and investigates the optimal demand response schedule that maximizes customer's net benefit. Chen *et al.* [18] propose stochastic optimization and robust optimization approaches for real-time price-based demand response management for residential appliances. Recently, Gangammanavar and Sen [19] present a stochastic optimization model of a power system comprised of distributed storage devices. To the best of our knowledge, only a few papers study the impact of network topology on managing energy systems and the system operator's perspective of energy management with demand response.

Recently, the application of multi-agent models in power

systems has attracted researchers' attention. Kumar Nunna and Dolla [20] propose a framework for distributed energy resource management for interconnected MGs using muti-agent systems such that various entities can participate in the market. Logenthiran *et al.* [21] use multi-agent systems for energy resource scheduling of an islanded power system with distributed generation. The authors use Lagrangian Relaxation with a Genetic Algorithm to analyze the problem. Unfortunately, both of these multi-agent approaches cannot provide a near optimal solution for systems with more than just three MGs.

In light of above contents, the main contributions of this paper are:

(a) A stochastic programming model that extends the classical two-stage formulation to accommodate multiple subproblems. In the power systems context, this model is designed for a centralized arbiter, who is charged with generating and supplying power to a set of utilities and MGs with various weights (priorities), in the main grid. Each MG is allowed to respond to the decision of the centralized arbiter and a stochastic realization of renewable generation. Our formulation also allows for different energy management systems to be operational at the MGs. This formulation is presented in §II.

(b) We extend the two-stage stochastic decomposition (2-SD) to solve models with multiple subproblems. Our approach, which we refer to as the multi-agent stochastic decomposition, is a decomposition-based sequential sampling algorithm. It dynamically identifies the number of samples required to characterize the uncertainty at a particular MG and provides statistically verifiable solutions and objective function estimates. We provide a brief description of our approach in §III. The computational results, presented in §IV, highlight the scalability of our algorithm to large-scale power systems.

II. Problem Formulation

We consider a power system that is comprised of a main grid connected to multiple MGs. A centralized arbiter monitors the activities of the main grid and its interactions with the MGs. This system uses both conventional and renewable energy resources to meet customer demand. Each entity in the system is exposed to varied sources of uncertainty (demand, renewable generation, etc.) and utilizes different energy management settings. Fig.1 shows the system we described above. To capture these properties of the system, we present a stochastic optimization formulation that is comprised of (a) an arbiter problem where decisions are made before the realization of any uncertainty and (b) multiple agent problems where decisions are made in response to their respective stochastic outcomes. This formulation is an extension of the classical 2-SP and will be referred to as the multi-agent stochastic program (MA-SP).

Let $\mathcal{N} = \{0, 1, 2, \ldots, N\}$ denote the set of agents in the system, where $n = 0$ corresponds to the main grid. Let $\mathcal{T} = \{0, 1, 2, \ldots, T\}$ denote the set of discrete time decision epochs. At time period t, customer demand at each agent can be met through local generation (conventional and renewable) as well as energy bought from the main grid (when $n \neq 0$). We first begin by presenting the arbiter's optimization problem.

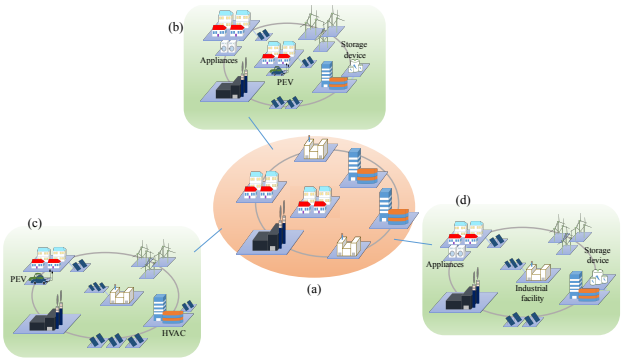

Fig. 1: A power system: A main grid (a) connects to multiple MGs ((b) - (d)) that utilize different energy management settings

A. Arbiter Problem

The centralized arbiter determines the conventional generation level at the main grid as well as its power transactions with all the MGs. The set of generators in the main grid is denoted by $\mathcal{G}_0$. For every generator $j \in \mathcal{G}_0$, the generation level and the corresponding cost are denoted by g_{0jt} and c^g_{0jt}, respectively. The transaction decisions b_{ijt} between the main grid and MGs are determined for all $(i, j) \in \mathcal{I}_n$ at a price of c^b_{ijt}, where $\mathcal{I}_n$ is the set of interconnection links. These generation and transaction decisions are made so as to satisfy the following power balance equation:

$$\sum_{j \in \mathcal{G}_0} g_{0jt} = \sum_{j \in \mathcal{D}_0 \bigcup \mathcal{R}_0} \partial \bar{D}_{0jt} + \sum_{(i,j) \in \mathcal{I}_n} b_{ijt} \quad \forall t \in \mathcal{T}, \quad (1)$$

where $\partial \bar{D}_{0jt}$ is the net demand computed using the forecasted demand ($\mathcal{D}_0$) and renewable generation ($\mathcal{R}_0$) in the main grid. In addition, generation and transaction decisions are bounded by their respective physical limits. Further, these decisions are established in a "here and now" manner and effect the state of every agent in the system. We will succinctly denote the arbiter's decision vector by $x = (x_t)_{t \in \mathcal{T}}$ and cost vector by $c = (c_t)_{t \in \mathcal{T}}$, where $x_t = ((g_{0jt})_{j \in \mathcal{G}_0}, (b_{ijt})_{(i,j) \in \mathcal{I}})$ and the corresponding cost coefficients by $c_t = ((c^g_{0jt})_{j \in \mathcal{G}_0}, (-c^b_{ijt})_{(i,j) \in \mathcal{I}})$. The feasible set characterised by (1) is denoted by $\mathcal{X}$. Once the arbiter makes its decision, each agent responds to this decision and a realization ω_n of its stochastic process $\tilde{\omega}_n$ at a recourse cost of $h_n(x, \omega_n)$. We assume that the stochastic processes affecting the agents are independent of each other.

The objective of the centralized arbiter is to minimize the energy cost and the sum of weighted expected recourse functions. Its optimization problem is given by:

$$\begin{aligned} &\min\ c^\top x + \sum_{n \in \mathcal{N}} v_n \mathbb{E}\{h_n(x, \omega_n)\} \\ &\text{s.t. } x \in \mathcal{X}, \end{aligned} \quad (2)$$

where the weight $v_n \geq 0\ \forall n \in \mathcal{N}$.

B. Agent problem

Each agent in the system, that is, the main grid and all MGs, is associated with an agent problem. This problem is characterized by the energy management setting adopted and stochasticity faced by the agent. The energy resources of an

agent n include the set of conventional generators $\mathcal{G}_n$ as well as renewable generators $\mathcal{R}_n$. The conventional generators at MGs ($n \neq 0$) usually have lower capacities when compared to the main grid ($n = 0$) generators. In addition to these local energy resources, the MGs can utilize a fraction of the energy available from the main grid. The generation levels $g_{0jt}\ \forall j \in \mathcal{G}_0$ at the main grid, which were set by the arbiter, are allowed to be updated.

These resources are used to meet customers demands, which are denoted by $\mathcal{D}_n$. Further, all customer demands can be categorized as fixed and flexible. The fixed demand, D_{njt}, at location $j \in \mathcal{D}_n^f$ must be met in the current time period t. In other words,

$$a_{njt} \geq D_{njt}, \tag{3}$$

where a_{njt} is the power utilized to meet this fixed demand. The flexible demand, $\mathcal{D}_n^v$, depends on the energy management settings adopted by each agent. We will describe these settings in the following.

1) Energy Management Settings: Each agent may adopt (one or more) different settings. Therefore, we omit the agent index n while presenting these settings.

(a) Industrial Sector: The field of production management provides flexibility in how demand at a particular facility can be met during the operation time horizon [15]. This, in turn, allows for efficiently utilizing the available energy resources. To ensure that the production demand is met, the cumulative power consumption within a production window must exceed a given threshold.

Let $\mathcal{V}^i$ denote a set of industrial facilities. If for each $j \in \mathcal{V}^i$, the time window within which the demand D_j^i can be satisfied is given by $[\underline{\tau}_j^i, \bar{\tau}_j^i] \subseteq \mathcal{T}$. This requirement is captured by:

$$\sum_{t \in [\underline{\tau}_j^i, \bar{\tau}_j^i]} a_{jt} \geq D_j^i. \tag{4}$$

In the above, a_{jt} is the realized power in time period t that is restricted to be within an interval $[a_j^{min},\ a_j^{max}] \in \mathbb{R}$. The equipment used in industrial settings are associated with significant start-up time and set-up cost. Therefore, it is efficient to run the industrial equipment uninterrupted, which is ensured by setting $a_j^{min} > 0$.

(b) Building Management: For commercial buildings, around 50% of the energy is consumed by heating, ventilation, and air conditioning (HVAC) systems to provide a comfortable indoor environment [22]. Let $\mathcal{V}^h$ denote the set of buildings that have intelligent HVAC systems. Since comfort is a qualitative term, it is best captured through a flexible range. For example, the comfortable indoor temperature ranges between 20°C to 25°C [23]. Moreover, this comfort is also associated with climate [24] and building occupancy [25]. For these reasons, the amount of energy consumed has a fixed minimum level D_{jt}^h (corresponding to the minimum comfort requirement) and a flexible portion Δ_{jt}^h for all $j \in \mathcal{V}^h$. The flexible portion can frequently fluctuate within a range without reducing the end-user's comfort significantly. This is ensured by:

$$D_{jt}^h \leq a_{jt} \leq D_{jt}^h + \Delta_{jt}^h \quad \forall j \in \mathcal{V}^h, \forall t \in \mathcal{T}. \tag{5}$$

Note that, while the demand in (4) can be met across multiple time periods, the demand here is time-dependent and should be met in its time period.

(c) Storage Devices: It has been identified that storage devices will play a critical role in mitigating renewable regulation challenges [26] [27]. Apart from energy arbitrage, storage devices can provide ancillary, capacity deferral and end-user services [28]. Let $\mathcal{V}^b$ denote a set of storage devices. For each $j \in \mathcal{V}^b$, a_{jt} is the charging/discharging amount during time period t. If this value is positive, it indicates a charging activity—discharging otherwise. These decisions are bounded by charging/discharging rates of the storage devices: $a_{jt} \in [a_j^{min}, a_j^{max}] \in \mathbb{R}$. Let s_{jt} denote the state of storage devices that is required to satisfy the following dynamics equation:

$$s_{jt} = s_{j,t-1} + a_{jt} \qquad \forall j \in \mathcal{V}^b,\ \forall t \in \mathcal{T}, \tag{6}$$

where the initial state s_{j0} is assumed to be given. This variable is also bounded by the capacity of this storage device, that is $0 \leq s_{jt} \leq s_j^{max}$. In any time period, a storage device can act both as source and sink of energy.

(d) Plug-in Electric Vehicle (PEV): The operating principle of PEVs is similar to that of storage devices. However, unlike the storage devices, the charging and discharging activities depend on the utility of the vehicle. For example, it should be expected that the PEVs are connected to a residential grid during the off-work hours. Therefore, the whole operation must be completed during a time period that is desired by the customer. Using similar definitions as given for storage devices, for $j \in \mathcal{V}_p$, the set of PEVs must satisfy:

$$a_j^{min} \leq a_{jt} \leq a_j^{max},\ s_j^{min} \leq s_{jt} \leq s_j^{max} \tag{7a}$$

$$s_{jt} = s_{j,t-1} + a_{jt} \quad \forall t \in [\underline{\tau}_j^p, \bar{\tau}_j^p], \tag{7b}$$

where $[\underline{\tau}_j^p, \bar{\tau}_j^p]$ is the plug-in interval. Further, the state of the PEVs at the end of the plug-in interval must satisfy the specific customer-desired requirement [18]:

$$s_{j\bar{\tau}_j^p} = S_j \quad \forall j \in \mathcal{V}^p. \tag{8}$$

(e) Home Appliances: The operation of some appliances, such as dishwashers and washing machines, is flexible over a time horizon. These appliances have relatively lower demand compared to the other settings described thus far. Let $\mathcal{V}^a$ denote a set of appliances. For each $j \in \mathcal{V}^a$, a_{jt} is the power utilized in time period t, which must satisfy:

$$\sum_{t \in [\underline{\tau}_j^a, \bar{\tau}_j^a]} a_{jt} \geq D_j^a \tag{9}$$

during the desired time window $[\underline{\tau}_j^a, \bar{\tau}_j^a]$. The operation of these appliances can withstand interruptions since the start-up time and set-up cost are negligible. Moreover, power utilized in any time period should be less than the power rating of the appliance. Therefore, $a_{jt} \in [0, a_j^{max}]$. The interruptible nature of these appliances differentiates them from industrial equipment.

We restrict our attention to the above five settings, but other similar settings can also be operated within our multi-agent framework. Moreover, for agent n the flexible demand set $\mathcal{D}_n^v$ can be any combination of the above settings. The feasible region for decisions a_{njt}, where $j \in \mathcal{D}_n^v$ depends on this combination and will be denoted as $\mathcal{A}_n^v$. For example, for a household with storage devices and PEV units installed, the set $\mathcal{D}_n^v = \mathcal{V}_n^b \bigcup \mathcal{V}_n^p \bigcup \mathcal{V}_n^a$. In this case, the feasible region $\mathcal{A}_n^v$ is characterized by (6), (7), (8) and (9) along with the respective bounds.

2) Power Network Constraints: The power grid in both the main grid and MGs consists of buses and lines that construct a network with a set of buses $\mathcal{B}_n$ and a set of transmission lines $\mathcal{L}_n$. At any bus $i \in \mathcal{B}_n$, the total available power should meet the total of fixed and flexible demands, thus, satisfying the following:

$$\sum_{j\in\mathcal{G}_{ni}} g_{njt} + \Big(\sum_{j:(j,i)\in\mathcal{L}_n} p_{njit} - \sum_{j:(i,j)\in\mathcal{L}_n} p_{nijt}\Big) - \sum_{j\in\mathcal{D}_{ni}} a_{njt} + \sum_{\substack{j:(j,i)\in\mathcal{I}_n,\\ n\neq 0}} u_{jit} = r_i(x_t,\tilde{\omega}_{nit}) \quad \forall t\in\mathcal{T}, \tag{10}$$

where p_{njit} and p_{nijt} are the flow into and out of bus i, respectively. Further, u_{jit} is the purchased power that is unused. Note that this variable appears only in MG problems. The right-hand side $r_i(x_t,\tilde{\omega}_{nit})$ depends on the arbiter's decision and the renewable generation $\tilde{\omega}_{nit}$. Note that the right-hand side $r_i(x_t,\tilde{\omega}_{nit})$ for the main grid and MGs are different since the main grid acts as a seller rather than a buyer in the transactions with agents. Therefore, for any bus $i \in \mathcal{B}_n$, $r_i(x_t,\tilde{\omega}_{nit})$ is set as the following:

$$r_i(x_t,\tilde{\omega}_{nit}) = \begin{cases} -\sum_{j\in\mathcal{R}_{ni}} \tilde{\omega}_{njt} + \sum_{j:(i,j)\in\mathcal{I}_n} b_{ijt} & \text{if } n=0 \\ -\sum_{j\in\mathcal{R}_{ni}} \tilde{\omega}_{njt} - \sum_{j:(j,i)\in\mathcal{I}_n} b_{jit} & \text{if } n\neq 0. \end{cases} \tag{11}$$

On any transmission line, the real transmitted power and power losses are non-linear functions of the differences between the voltages and angles of buses in both ends of connecting lines. To make theses functions suitable for linear optimization methods, we apply a linear approximation described in [29]. We ignore the power flow losses. If V_{nit} denotes the voltage of bus i, and X_{nij} denotes the reactance of line $(i,j)\in\mathcal{L}_n$, then the power flow p_{nijt} is given by:

$$p_{nijt} = \frac{V_{nit}V_{njt}}{X_{nij}}(\theta_{nit}-\theta_{njt}) \quad \forall t\in\mathcal{T}, \tag{12}$$

where the decision variable θ_{nit} is the angle of bus i. Further, the power flow p_{nijt} and bus angle θ_{nit} should be within their intervals $[p^{min}_{nij}, p^{max}_{nij}]$ and $[\theta^{min}_{nij}, \theta^{max}_{nij}]$, respectively.

Each agent has an objective minimizing the total cost of generation and the penalty for under-utilizing the power already purchased. Let c^g_{njt} and c^u_{ijt} represent the corresponding unit costs, thus, the objective is:

$$\begin{aligned} h_n((x_t),\omega_{nt}) = \min \sum_{t\in\mathcal{T}_n}\Big[\sum_{j\in\mathcal{G}_n} c^g_{njt}g_{njt} + \sum_{\substack{(i,j)\in\mathcal{I}_n\\ n\neq 0}} c^u_{ijt}u_{ijt}\Big] \\ s.t.\ (3),\ (10), \text{and } (12) \\ a_{njt}\in\mathcal{A}^v_n. \end{aligned} \tag{13}$$

The arbiter's decision as well as stochastic information (renewable generation) effect only the right-hand side of the above program. Note that this is also the case for the subproblem of the classical 2-SP with fixed recourse:

$$\begin{aligned} h_n(x,\omega_n) = \min\ & g_n^\top y_n \\ s.t.\ & W_n y_n \le r_n(\omega_n) - T_n(\omega_n)x, y_n \ge 0. \end{aligned} \tag{14}$$

For easy notation, we will use the above representation of the subproblem to present our algorithm. The arbiter's problem in (2), henceforth referred to as the first-stage problem, and the agent subproblem in (13) together constitute our MA-SP.

III. Algorithm

The formulation introduced in §II has an arbiter problem where decisions are made before the realization of demand and renewable generation as well as multiple agent problems that provide the recourse costs for the arbiter's selection. While this decision structure is similar to 2-SPs, the presence of multiple subproblems distinguishes our MA-SP from the classical formulation. Moreover, the subproblems have heterogeneous optimization problems and are exposed to different stochastic processes.

The classical 2-SPs are well studied in the literature. Several algorithms have been proposed, notably, Benders' decomposition [30], Dantzig-Wolfe decomposition [31], and progressive hedging [32]. These algorithms approximate the expected recourse function using piecewise linear functions. These approximations are created by solving a subproblem for each scenario from a set of scenarios selected a priori. For large-scale problems and/or problems with a large set of scenarios, such enumeration can prove to be computationally challenging. This is particularly the case in power systems with significant renewable integration. For such problems, sequential sampling-based bundling algorithms, such as 2-SD, have proven to be effective [14]. Motivated by their observations, we adopt a modified 2-SD solution approach to tackle our MA-SP.

Our solution approach, which we refer to as multi-agent stochastic decomposition (MA-SD), is an extension of 2-SD when multiple subproblems exist. The principal idea is to use a separate sample mean function to approximate the expected recourse function for each agent in (2):

$$H^k_n(x) = \frac{1}{k}\sum_{j\in\Omega^k_n} h_n(x,\omega^j_n) \qquad \forall n\in\mathcal{N}. \tag{15}$$

Note that, the above sample mean is based on the current set of observations Ω^k_n. In any iteration k, these sample mean functions are updated by sequentially sampling scenarios (ω^k_n) from their respective stochastic processes and updating the observation set Ω^k_n. For the current arbiter decision x^k and newly sampled observation ω^k_n, the subproblem for agent-n is solved. Let π^{kk}_n denote the corresponding optimal dual solution. This solution is added to the set of previously encountered dual solutions, Π^k_n. For the remaining observations $\omega^j_n \in \Omega^k_n$, a dual solution π^{kj}_n is identified in Π^k_n, which provides the best lower bound at x^k. Using these dual solutions $\{\pi^{kj}_n\}^k_{j=1}$, we compute a lower bounding affine function for the k^{th} sample mean function $H^k_n(x)$:

$$H^k_n(x) \ge \underbrace{\frac{1}{k}\sum_{j=1}^{k}(\pi^{kj}_n)^\top[r_n(\omega^j_n) - T_n(\omega^j_n)x]}_{:=\ \ell^k_n(x,\Omega^k_n)}. \tag{16}$$

Note that $H^k_n(x)$ approaches the expectation function as $k\to\infty$. Further, the affine function ℓ^j_n computed in iteration $j(<k)$ is a lower bound for H^j_n, and not necessarily for H^k_n. Therefore, the previously generated affine functions are updated by multiplying ℓ^j_n by the factor $\frac{j}{k}$. Using these, the piecewise linear approximation [33] of the expected recourse function of agent n is given by:

$$L^k_n(x) = \max_{j=1,\dots,k}\left\{\frac{j}{k}\times\ell^j_n(x,\Omega^k_n)\right\}. \tag{17}$$

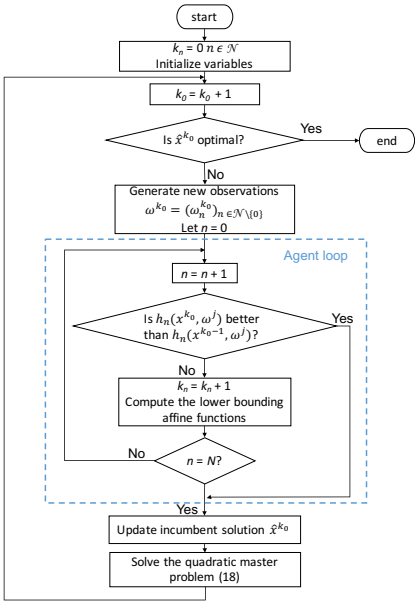

Fig. 2: Flowchart of the MA-SD algorithm

Approximations of (17) are weighted and aggregated across all agents to form the first-stage problem, which is given by

$$\min \ \{c^\top x + \sum_{n=1}^{N} v_n L_n^k(x) + \frac{\sigma^k}{2}||x - \hat{x}^k||^2 \ | x \in \mathcal{X}\}, \quad (18)$$

for a given parameter $\sigma^k > 0$. The optimal solution of the above problem x^{k+1} will be used in the subsequent iteration. Notice the use of a regularization term, centered around the incumbent solution $\hat{x}^k$, in the objective function. This term is included to stabilize our sampling-based approach. We refer the reader to for a detailed exposition of incumbent updates and convergence properties of our approach. Fig. 2 provides a flowchart representation of our algorithm.

Since each agent is exposed to an independent stochastic process, one should expect that different number of scenarios are required to characterize the uncertainty. Further, since the optimization problem is different at every agent, the number of extreme points (dual solutions) relevant to approximate the cost function is also different. In this regard, our stopping rules are based on in-sample as well as out-sample tests for stability of the observation set Ω_n^k and dual solution set Π_n^k. We refer the reader to [34] for more details. Due to the heterogeneous nature of decision processes, different agents might satisfy the stopping criteria at different iterations. Further, since the algorithm allows samples to be added sequentially during the optimization process, such a sequence can be obtained from state-of-the-art simulators that are often used by power system operators.

IV. Computational Experiment

For our computational experiments, we used the WECC-240 data set obtained from [35]. The data consists of a detailed description of network topology, generator location, and capacity. We decomposed the network into one main grid connected to 10 MGs (i.e. $N = 10$). In this data set, renewable generators and flexible demands are located only in the MGs. The renewable generation data was extracted from the Western Wind and Solar Integration Study [36] based on the generators' geographical locations. This data was scaled to ensure 15% renewable penetration at each MG. The flexible demand buses were selected randomly from the set of all load buses. We adopted the generation costs provided by [37]. Table I presents the details of this power system. In our computational study, we set the time horizon $T = 24$ hours.

All algorithms were implemented in the C programming language on a 64-bit Intel core i7-4770 CPU @3.4GHz $\times$ 8 machine with 32 GB Memory. All linear and quadratic programs were solved using CPLEX callable subroutines. In all our experiments, we begin by using an optimization process to identify an optimal solution for the arbiter and the corresponding prediction value. Note that this prediction value is an estimate of the lower bound for the original optimization problem. This is followed by a verification phase where the arbiter's solution is fixed, and agents (MGs) subproblems are simulated using independent and identically distributed observations. The objective functions obtained are used to build a confidence interval (CI) of the upper bound estimate for each agent's expected recourse function. The CI for the arbiter objective function value is the aggregate based on the weighted sum of individual agent objective values.

A. Comparison of Formulations

We start by comparing our MA-SP with the classical 2-SP. While MA-SP includes a separate subproblem for each agent, the 2-SP considers a subproblem that aggregates together the decision processes of all agents. The first-stage problem in both these formulations remains the same. We used the 2-SD algorithm to optimize the 2-SP. These results are summarized in Table II.

Note that the prediction value for MA-SP is within 0.5% of that predicted by the benchmark 2-SD algorithm. This indicates that the objective function value estimated by considering a separate sampling procedure for each agent is statistically

Program	# LPs	Prediction	Time/iter	Verification CI	p-value
2-SP	708	43,760,652	18.682	[43,499,527, 44,103,080]	-
MA-SP	670	43,951,145	9.849	[43,534,253, 44,252,131]	0.7008

TABLE II: Comparison between 2-SP and MA-SP

Agent	Weights	Buses	Lines	Generators		Loads		Energy Management Settings				
				Conventional	Renewable	Fixed	Flexible	Industrial Sectors	Building Managements	Storage Devices	PEV	Home Appliances
0	1	81	100	24	0	40	0	0	0	0	0	0
1	1	21	24	15	3	7	6	2	1	1	1	1
2	1	2	1	2	1	0	1	0	0	0	0	1
3	1	15	18	2	1	5	7	2	1	1	2	1
4	1	14	17	3	1	3	7	2	1	0	2	2
5	1	29	36	5	1	12	11	3	1	2	3	2
6	1	33	41	16	7	5	10	3	1	1	2	3
7	1	6	5	5	1	0	3	2	0	0	0	1
8	1	29	36	17	4	11	10	2	3	1	3	1
9	1	5	4	3	1	1	2	0	0	0	1	1
10	1	5	5	3	1	1	3	1	0	0	1	1

TABLE I: Details of the WECC-240 power system

Agent	MA-SD(a)						MA-SD(m)						p-value
	#of optimization programs	Time per iter. (s)	Prediction value	U.B. Estimate Mean	Std. dev.	95% C.I.	#of linear programs	Time per iter. (s)	Prediction value	U.B. Estimate Mean	Std. dev.	95% C.I	
master	670	9.849	43,951,145	43,893,192	5,788,250	[43,534,253, 44,252,131]	435	15.957	44,066,906	43,885,109	5,796,994	[43,525,628, 44,244,591]	0.9751
0	369	0.012	0.007	0.007	0.000	[0.007, 0.007]	311	0.012	0.004	0.004	0.000	[0.004, 0.004]	-
1	301	0.002	8,998,948	8,997,077	150,725	[8,987,730, 9,006,424]	279	0.002	8,657,521	8,654,370	142,600	[8,645,527, 8,663,213]	-
2	475	0.002	8,755	8,749	694	[8,706, 8,792]	433	0.002	8,824	8,790	723	[8,745, 8,834]	-
3	359	0.004	2,139,078	2,140,098	91,629	[2,134,416, 2,145,780]	375	0.003	2,144,479	2,146,895	98,548	[2,140,784, 2,153,006]	-
4	343	0.004	2,076,822	1,994,509	946,845	[1,935,793, 2,053,224]	346	0.004	2,053,008	2,008,981	958,127	[1,949,566, 2,068,396]	-
5	368	0.015	783,400	772,364	310,294	[753,122, 791,606]	393	0.019	800,002	774,888	311,272	[755,585, 794,190]	-
6	275	0.014	4,263,634	4,205,003	2,863,423	[4,027,438, 4,382,569]	267	0.017	4,426,207	4,213,061	2,870,708	[4,035,044, 4,391,078]	-
7	374	0.003	5,228,603	5,350,485	4,560,169	[5,067,701, 5,633,268]	314	0.002	5,173,337	5,341,604	4,560,194	[5,058,819, 5,624,389]	-
8	265	0.006	6,692,126	6,665,261	1,822,699	[6,552,233, 6,778,290]	263	0.007	7,025,171	6,965,143	1,830,957	[6,851,602, 7,078,684]	-
9	323	0.001	206,019	203,565	101,432	[197,275, 209,855]	317	0.001	197,412	192,457	92,595	[186,715, 198,199]	-
10	351	0.002	645,443	640,605	220,237	[626,947, 654,262]	281	0.001	648,653	646,629	222,103	[632,856, 660,402]	-

TABLE III: Comparison of MA-SD(a) and MA-SD(m)

similar to when a single stream of samples is used. The verification CIs, on the other hand, provide us with a tool to compare the solutions generated from the formulations. We accomplished this by testing the following hypothesis: the solutions from the two formulations are statistically indistinguishable. The p-value associated with this hypothesis test is 0.7008, which is greater than 0.05. It indicates that the hypothesis cannot be rejected at a 0.95 significance level. Further, the average time taken to complete an iteration of each algorithm is presented in Table II as well. Since MA-SP decomposes the subproblems into smaller linear programs, the computational requirements are lower when compared to 2-SP where a significantly larger linear program is solved. Therefore, the average time taken for an iteration in 2-SD is twice as much as MA-SD. The separation of sampling procedures and the computational advantage make the MA-SP setup suitable for parallel computing environments. We are currently working on an implementation suitable for such environments, and the results will be reported in future publications.

B. Comparison of Cut Formation Procedures

The expected recourse function for each agent is approximated using lower bounding affine functions as described in §III. These approximations are included in the master problem as linear functional constraints [38]. This implies that the size of the master problem grows by N (number of agents/MGs) in every iteration that increases the computational burden of solving quadratic programs. Alternatively, one may aggregate these affine functions as:

$$\bar{\alpha} = \sum_{n=1}^{N} v_n \alpha_n; \qquad \bar{\beta} = \sum_{n=1}^{N} v_n \beta_n, \tag{19}$$

where (α_n, β_n) are coefficients of individual affine functions for $n = 1, \ldots, N$, and $(\bar{\alpha}, \bar{\beta})$ are those for the aggregated affine function. This choice motivates the next set of experiments where we compare the MA-SD(m) and MA-SD(a) procedures. In MA-SD(m), N affine functions are added in every iteration, and a single aggregated function is added in MA-SD(a). The comparison results are shown in Table III.

These results indicate that, while the number of quadratic master programs solved is higher in the case of MA-SD(a) when compared to MA-SD(m), the corresponding running time is lower. This can be attributed to the larger size of the master problem in the MA-SD(m). As before, we can compare the prediction and verification values to establish the similarity between the two approaches. The difference in prediction values of the two approaches is around 0.3%. The p-value of 0.9751 (> 0.05) indicates that we can not reject the null hypothesis of statistically indistinguishable arbiter solutions.

The results in the table showcase one of the principal features of our solution approach, viz. the distributed nature of our sequential sampling procedure. Since each agent is exposed to stochastic processes with different characteristics (mean, variance, etc.), the number of samples required to satisfactorily approximate the expected recourse function is also different. These numbers can be seen in the first column of TABLE III for each method. For sample-based stochastic programming models, it is not guaranteed that the prediction value falls within the verification CI. However, when it does, then the solutions can be accepted with greater confidence. The arbiter solution satisfies this condition as the aggregated prediction value falls within the verification CI for both methods proposed. (See the row corresponding to "master" in TABLE III). While this solution is statistically acceptable to the aggregated optimization problem, it might not be the case for individual agents (e.g., agent 4 in the MA-SD(a) method). Such behavior can be attributed to the fact that our approach seeks solutions that are optimal across all and not necessarily individual agents. In the remaining experiments, we will use MA-SD(a) as our method of choice to solve MA-SPs.

C. Energy Management Study

The formulation of the power system presented in §II permitted different energy management settings to be included at the agents. A main feature of these settings was the flexibility to schedule demand in a way that reduces overall system costs by efficiently managing their schedule with availabilities of renewable resources. In order to quantify the cost savings, we designed an experiment to compare a system with/without such flexible demands. Our experiment used two small instances comprised of agents 0, 4, 9, and 10 (all without storage devices)—one instance has inflexible customer demands and

Instances	Prediction Value	Conventional Generation (MW)	Selling Power (MW)	Verification C.I.	p-value
Fixed	6,360,378	412,471	108,236	[6,316,083, 6,364,164]	-
Flexible	4,879,788	376,221	71,986	[4,818,633, 4,867,403]	0

TABLE IV: Solution method comparison (Fixed and Flexible)

the other instance allows flexibility. All renewable generation scenarios used in this experiment are from the same data set as before.

The prediction and verification results are summarized in Table IV. The prediction values indicate that incorporating flexibility in energy management systems helps to reap more benefits from renewable resources and thereby results in cost savings (23.3%). This decrease in cost can be attributed to an 8.8% reduction in the conventional generation and a 33.5% reduction in the total amount of energy sold by the main grid. When demand is allowed to be flexible, it is scheduled to be met during time periods of high renewable generation. This allows us to efficiently utilize the renewable resources and thereby reduce the dependence on conventional energy resources. Moreover, our sampling-based approach provides an effective tool to accurately capture the response of flexible demand to a large set of renewable generation scenarios. This large set of responses (recourse decisions in our model) in turn guides the optimization process used to identify the arbiter's decision (master problem).

D. Response of Flexible Demands

In this experiment, we study the response of flexible demands to fluctuations in renewable generation over the planning horizon. The optimal first-stage solution identified by MA-SD(a) is treated as an input to the individual agent problem. The decision process of each agent is simulated by solving an optimization problem using independent Monte-Carlo samples. Some key observations are discussed here.

Fig. 3 shows the mean responses over 1000 samples for different settings during a day for agents 1, 3, and 6. The power purchased (which is a part of arbiter decisions), local conventional generation, and renewable generation, are utilized to satisfy both flexible and fixed demand of an agent. During time window [0, 9], the requirements of industrial facilities dominate the power consumption and drive a high level of local conventional generation for all the three agents. In time period 10, when the industrial facilities stop operating, the local conventional generation reduces dramatically while the purchased power increases for agents 1 and 3 only.

Another interesting observation from Fig. 3 is that industrial and home appliances demand realization trends complement one another. For example, when industrial demand decreases at the end of time period 9, the demand of home appliances is scheduled to be met. This behavior can be attributed to the fact that home appliances are allowed to operate over a longer time window as compared to industrial demand, which makes them more flexible. Similar complementary behavior was observed between conventional and renewable generation. We also can see from Fig. 3 that excess renewable energy is stored (e.g., in $t \geq 10$ in agent 6) for future usage. While the realized power for the HVACs is constant for a majority of agents, this is not the case for agent 6 (see Fig. 3). This is due to the presence of renewable resources with higher variability at this agent when compared to others. Both HVACs and storage devices help in smoothing this variability.

V. Conclusion

In this paper, we presented a stochastic optimization framework that captures interactions between (a) a centralized arbiter in the main grid and (b) multiple agents with heterogeneous objectives and constraints in MGs that utilize various energy management settings. We investigated the response of each agent to intermittent renewable resources by extending the classical 2-SP model to include multiple subproblems. To the best of our knowledge, this is the first study that investigates multiple subproblems with heterogeneous decisions and stochastic processes in the second-stage. We developed stochastic decomposition-based algorithms to solve the proposed large-scale problem. The statistical results showed that

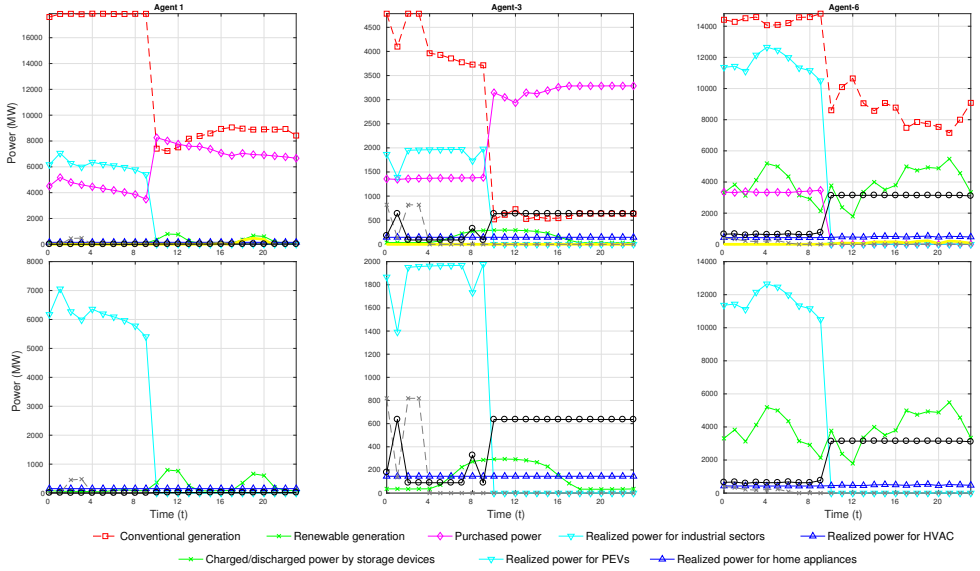

Fig. 3: Mean agent response for different energy management settings

our algorithm can provide reliable overall cost estimates to the proposed problem with 50% less running time as compared to our benchmark 2-SD approach. The results implemented with and without allowing flexible demands show that the total operational costs can be reduced significantly when customer demand is flexible by effective utilization of the renewable resources. Finally, we studied how the activities of these flexible demands fluctuate with variations of renewable generations during a day.

The structure of our algorithm involves solving several independent subproblems (corresponding to MGs). This structure is naturally fit for an implementation of distributed/parallel computing, which will be taken up as part of our future study. In a smart grid, MGs not only are buyers but also can sell power back to the main grid to increase utilization of renewable energy over the entire power system. Furthermore, they are allowed to make transactions with other MGs in the system as well. These features will also be addressed in our future work.

REFERENCES

[1] Y. Chen, S. Lu, Y. Chang, T. Lee, and M. Hu, "Economic analysis and optimal energy management models for microgrid systems: A case study in Taiwan," *Applied Energy*, vol. 103, pp. 145–154, 2013.

[2] P. Basak, S. Chowdhury, S. Halder nee Dey, and S.P. Chowdhury, "A literature review on integration of distributed energy resources in the perspective of control, protection and stability of microgrid," *Renewable and Sustainable Energy Reviews*, vol. 16, no. 8, pp. 5545–5556, 2012.

[3] A. Zakariazadeh, J. Shahram, and P. Siano, "Smart microgrid energy and reserve scheduling with demand response using stochastic optimization," *International Journal of Electrical Power & Energy Systems*, vol. 63, pp. 523–533, 2014.

[4] D. Nguyenand and L. B. Le, "Optimal energy management for cooperative microgrids with renewable energy resources," in *Smart Grid Communications (SmartGridComm), 2013 IEEE International Conference on*. IEEE, 2013, pp. 678–683.

[5] T. Ackermann, G. Andersson, and L. Söder, "Distributed generation: a definition," *Electric Power Systems Research*, vol. 57, no. 3, pp. 195–204, 2001.

[6] G. Pepermans, J. Driesen, D. Haeseldonckx, R. Belmans, and W. D'haeseleer, "Distributed generation: definition, benefits and issues," *Energy Policy*, vol. 33, no. 6, pp. 787–798, 2005.

[7] N. Hamsic, A. Schmelter, A. Mohd, E. Ortjohann, E. Scheultze, A. Tuckey, and J. Zimmermann, "Increasing renewable energy penetration in isolated grids using a flywheel energy storage system," in *Power Engineering, Energy and Electrical Drives, 2007. POWERENG 2007. International Conference on*. IEEE, 2007, pp. 195–200.

[8] I. Stadler, "Power grid balancing of energy systems with high renewable energy penetration by demand response," *Utilities Policy*, vol. 16, no. 2, pp. 90–98, 2008.

[9] A. Evans, V. V. Strezov, and T. J. Evans, "Assessment of utility energy storage options for increased renewable energy penetration," *Renewable and Sustainable Energy Reviews*, vol. 16, no. 6, pp. 4141–4147, 2012.

[10] C. Bueno and J. A. Carta, "Wind powered pumped hydro storage systems, a means of increasing the penetration of renewable energy in the Canary Islands," *Renewable and Sustainable Energy Reviews*, vol. 10, no. 4, pp. 312–340, 2006.

[11] R. Segurado, G. Krajačić, N. Duić, and L. Alves, "Increasing the penetration of renewable energy resources in S. Vicente, Cape Verde," *Applied Energy*, vol. 88, no. 2, pp. 466–472, 2011.

[12] W. Su, J. Wang, and J. Roh, "Stochastic energy scheduling in microgrids with intermittent renewable energy resources," *IEEE Transactions on Smart Grid*, vol. 5, no. 4, pp. 1876–1883, 2014.

[13] Z. Wang, B. Chen, J. Wang, M. M. Begovic, and C. Chen, "Coordinated energy management of networked microgrids in distribution systems," *IEEE Transactions on Smart Grid*, vol. 6, no. 1, pp. 45–53, 2015.

[14] H. Gangammanavar, S. Sen, and V. M. Zavala, "Stochastic optimization of sub-hourly economic dispatch with wind energy," *IEEE Transactions on Power System*, vol. 31, no. 2, pp. 949–959, 2015.

[15] Y. M. Ding, S. H. Hong, and X. H. Li, "A demand response energy management scheme for industrial facilities in smart grid," *IEEE Transactions on Industrial Informatics*, vol. 10, no. 4, pp. 2257–2269, 2014.

[16] G. Goddard, J. Klose, and S. Backhaus, "Model development and identification for fast demand response in commercial HVAC systems," *IEEE Transactions on Smart Grid*, vol. 5, no. 4, pp. 2084–2092, 2014.

[17] N. Li, L. Chen, and S. H. Low, "Optimal demand response based on utility maximization in power networks," in *2011 IEEE power and energy society general meeting*. IEEE, 2011, pp. 1–8.

[18] Z. Chen, L. Wu, and Y. Fu, "Real-time price-based demand response management for residential appliances via stochastic optimization and robust optimization," *IEEE Transactions on Smart Grid*, vol. 3, no. 4, pp. 1822–1831, 2012.

[19] H. Gangammanavar and S. Sen, "Two-scale stochastic optimization framework for controlling distributed storage devices," *IEEE Transactions on Smart Grid*, 2016.

[20] H.S.V.S. Kumar Nunna and S. Doolla, "Multiagent-based distributed-energy-resource management for intelligent microgrids," *IEEE Transactions on Industrial Electronics*, vol. 60, no. 4, pp. 1678–1687, 2013.

[21] T. Logenthiran, D. Srinivasan, and A. M. Khambadkone, "Multi-agent system for energy resource scheduling of integrated microgrids in a distributed system," *Electric Power Systems Research*, vol. 81, no. 1, pp. 138–148, 2011.

[22] P. Zhao, S. Suryanarayanan, and M. G. Simoes, "An energy management system for building structures using a multi-agent decision-making control methodology," *IEEE Transactions on Industry Applications*, vol. 49, no. 1, pp. 322–330, 2013.

[23] R. de Dear and G. S. Brager, "The adaptive model of thermal comfort and energy conservation in the built environment," *International Journal of Biometeorology*, vol. 45, no. 2, pp. 100–108, 2001.

[24] D. J. Sailor and A. A. Pavlova, "Air conditioning market saturation and long-term response of residential cooling energy demand to climate change," *Energy*, vol. 28, no. 9, pp. 941–951, 2003.

[25] Y. Agarwal, B. Balaji, R. Gupta, J. Lyles, M. Wei, and T. Weng, "Occupancy-driven energy management for smart building automation," in *Proceedings of the 2nd ACM Workshop on Embedded Sensing Systems for Energy-Efficiency in Building*. ACM, 2010, pp. 1–6.

[26] A. Etxeberria, I. Vechiu, H. Camblong, and J. M. Vinassa, "Hybrid energy storage systems for renewable energy sources integration in microgrids: A review," in *IPEC, 2010 Conference Proceedings*. IEEE, 2010, pp. 532–537.

[27] P. Denholm, E. Ela, B. Kirby, and M. Milligan, "The role of energy storage with renewable electricity generation," Tech. Rep., 2010, NREL/TP-6A247187 National Renewable Energy Laboratory.

[28] R. Sioshansi, P. Denholm, and T. Jenkin, "Market and policy barriers to deployment of energy storage," *Economics of Energy & Environmental Policy*, vol. 1, no. 2, pp. 47–63, 2012.

[29] A. L. Motto, F. D. Galiana, A. J. Conejo, and J. M. Arroyo, "Network-constrained multiperiod auction for a pool-based electricity market," *IEEE Transactions on Power Systems*, vol. 17, no. 3, pp. 646–653, 2002.

[30] J. F. Benders, "Partitioning procedures for solving mixed-variables programming problems," *Numerische Mathematik*, vol. 4, no. 1, pp. 238–252, 1962.

[31] G. B. Dantzig and P. Wolfe, "Decomposition principle for linear programs," *Operations Research*, vol. 8, no. 1, pp. 101–111, 1960.

[32] R. T. Rockafellar and R. J. B. Wets, "Scenarios and policy aggregation in optimization under uncertainty," *Mathematics of Operations Research*, vol. 16, no. 1, pp. 119–147, 1991.

[33] J. Higle and S. Sen, "Finite master programs in regularized stochastic decomposition," *Mathematical Programming*, vol. 67, no. 1-3, pp. 143–168, 1994.

[34] S. Sen and Y. Liu, "Mitigating uncertainty via compromise decisions in two-stage stochastic linear programming: variance reduction," *Operations Research*, vol. 64, no. 6, pp. 1422–1437, 2016.

[35] J. E. Price and J. Goodin, "Reduced network modeling of wecc as a market design prototype," in *2011 IEEE Power and Energy Society General Meeting*. IEEE, 2011, pp. 1–6.

[36] NREL. Western wind and solar integration study. Accessed: 2016-11-26. [Online]. Available: http://www.nrel.gov/grid/wwsis.html

[37] U.S.EIA. (2015) Levelized cost and levelized avoided cost of new generation resources in the annual energy outlook 2015. Accessed: 2016-11-26. [Online]. Available: http://www.eia.gov/outlooks/archive/aeo

[38] J. L. Higle and S. Sen, "Duality and statistical tests of optimality for two stage stochastic programs," *Mathematical Programming*, vol. 75, no. 2, pp. 257–275, 1996.